



## Development of multi-component fluoropolymer based coating on simulated outdoor patina on quaternary bronze

Tadeja Kosec<sup>a,\*</sup>, Luka Škrlep<sup>a</sup>, Erika Švara Fabjan<sup>a</sup>, Adrijana Sever Škapin<sup>a</sup>, Giulia Masi<sup>b</sup>, Elena Bernardi<sup>c</sup>, Cristina Chiavari<sup>d</sup>, Claudie Josse<sup>e</sup>, Jérôme Esvan<sup>f</sup>, Luc Robbiola<sup>g</sup>

<sup>a</sup> Slovenian National Building and Civil Engineering Institute, Dimičeva 12, 1000 Ljubljana, Slovenia

<sup>b</sup> Dipartimento di Ingegneria Civile, Chimica, Ambientale e dei Materiali, Università di Bologna, via Terracini, 28, 40131 Bologna, Italy

<sup>c</sup> Dipartimento di Chimica Industriale "Toso Montanari", Università di Bologna, via del Risorgimento, 4, 40136 Bologna, Italy

<sup>d</sup> Dipartimento di Beni Culturali, Università di Bologna, via degli Ariani, 1, 48121 Ravenna, Italy

<sup>e</sup> Centre de Microcaractérisation Raimond Castaing (CNRS UMS 3623), Université Fédérale de Toulouse, 31000 Toulouse, France

<sup>f</sup> Centre Interuniversitaire de Recherche et d'Ingénierie des Matériaux, Université de Toulouse, 4 allée Emile Monso, 31030 Toulouse, France

<sup>g</sup> TRACES lab (CNRS UMR5608), Université Toulouse Jean-Jaurès, 5, allées Antonio-Machado, 31058 Toulouse, France

### ARTICLE INFO

#### Keywords:

Bronze  
Aged patina  
Fluoropolymer coating  
Outdoor exposure  
Run-off condition

### ABSTRACT

Bronze reacts with oxygen, humidity, and pollutants in the atmosphere so that a patina forms. Natural exposure to an outdoor atmosphere can be simulated and accelerated in order to achieve a patina that mimics outdoor ancient patina. In order to avoid the uncontrolled dissolving of either the natural or artificially formed patina, protection of the patina is needed.

In this study, a multi-component fluoropolymer based coating for the protection of bronze patina was developed. In order to provide various functionalities of the coating (such as the hydrophobicity of the coating surface, obtaining interactions within the coating itself as well as a bronze substrate and inhibiting the corrosion processes), a fluoroacrylate coating with appropriate adhesion promoter was suggested, with and without a silane modified benzotriazole inhibitor. The protective efficiency and durability of the applied coatings were investigated electrochemically using potentiodynamic tests and electrochemical impedance spectroscopy in a simulated acid rain solution. All of the developed coatings showed a significant decrease in the corrosion current density. The self-assembled single layer coating (FA-MS) also showed 100% inhibition efficiency. After ageing the coating remained transparent and did not change by UV exposure and/or thermal cycling. The patina and coating investigations using FIB-SEM and EDX showed that the latter coating (FA-MS) successfully covered the surface of the patinated bronze. The mechanism of the bonding was proposed and supported with the spectroscopic observation of a thin and even coating.

### 1. Introduction

In order to avoid the dissolving of either natural or artificially formed patinas [1], various protective methods have been applied in practice, the most common being: waxes (bees wax, microcrystalline wax, Carnauba wax), lacquers (Incralac, Paraloid B44), and, occasionally, inhibitors dissolved either in wax or in lacquers [2].

There have been many reports about the inappropriate properties of Paraloid (a thermoplastic acrylic resin) which is frequently used in conservation practice [3–10]. It was reported that it decays quickly, especially when used on artificially patinated bronze [11]. In this study the aim was to develop a new, non-hazardous and efficient coating for outdoor exposed patinated bronze surfaces.

Fluoropolymer based coatings on bronze were investigated back in 2003 [12]. These particular coatings were tested on bare bronze as a new protective coating for the use on outdoor bronze monuments. Tests were performed on Incralac in different combinations of waxes and coatings based on hydrophobic fluoro-organic polymers. It was reported that microbes could biodegrade the Incralac finish [12]. On the other hand, in the case of fluoropolymer coatings, apart from good protective properties, the lack of adhesive properties was addressed as the main drawback of such polymer coatings [12]. The recent report on comparison of performance of protective coating for outdoor bronze included, beside multiple traditional and innovative coatings, fluoropolymer coating on bare and patinated bronze and by the use of benzotriazole as the pretreatment [13]. The fluoropolymer coating was

\* Corresponding author.

E-mail address: [tadeja.kosec@zag.si](mailto:tadeja.kosec@zag.si) (T. Kosec).

<https://doi.org/10.1016/j.porgcoat.2019.01.040>

Received 9 October 2018; Received in revised form 4 January 2019; Accepted 21 January 2019

Available online 23 February 2019

0300-9440/© 2019 The Authors. Published by Elsevier B.V. This is an open access article under the CC BY-NC-ND license (<http://creativecommons.org/licenses/by-nc-nd/4.0/>).

more efficient on patinated bronze [13].

The results of a literature search for fluoropolymer coatings currently under development have revealed their very versatile use for different applications in aeronautics, electronics, and marine applications as an anti-fouling agent. Fluoropolymer coatings have been reported to have anti-fouling properties when tested for mussel-controlled growth [14]. Also, fluoropolymer coatings have been shown to extend the shelf life of printed circuit copper boards by preventing oxidation and corrosion [15]. Fluoropolymer coatings have also been deposited by the chemical vapour method on copper surfaces; they exhibited super-hydrophobic properties with contact angles greater than  $160^\circ$  [16]. A perfluoroalkoxy composite polymer has been applied to different metallic materials, with the aim of achieving a high thermal conductivity and a low corrosion rate [17].

Fluoropolymers have many favourable properties with regard to corrosion protection such as low electrical conductivity, high hydrophobicity, and good barrier properties, as well as high photo, thermal and chemical stability. Their disadvantages are: a low dielectric constant, low adhesion, and limited solubility [18].

Due to the poor adhesion properties of fluoropolymers with mostly fluoro-carbon functionality such as PTFE and PVDF, fluoroacrylate (FA) was selected as a basis for coating development. Schematic presentation of the possible bonding of the proposed multi-component coating on aged bronze is presented in Fig. 1. Apart from fluoro-carbon functionality, it possesses additional functionalities such as an ester group which can contribute to better adhesion. In order to further enhance adhesion to bronze surfaces, adhesion promoters based on silane modified methacrylic polymer (MS) were specifically prepared. Methyl methacrylate including 3-methacryloxypropyltrimethoxysilane, with either 5 or 10 mol % of silane monomer, was used. Additionally, a

benzotriazole derivative (BS) was synthesised and tested.

The aim of this work is to present the development and evaluation of protective coatings on artificially patinated quaternary bronze, in order to find an effective solution for the protection of bronze surfaces when exposed to an aggressive outdoor environment. Since the functionalities of the coating such as the hydrophobicity of the surface, achieving interactions within the coating itself, as well as with the bronze substrate and inhibition of corrosion, are expected, it was suggested that the following multi-component fluoropolymer based coating be used: a fluoroacrylate coating (FA) with an appropriate adhesion promoter (MS), with and without a silane modified benzotriazole inhibitor (BS). Two different application techniques were planned: (i) with single layer application of all the pre-mixed components (in this case the proposed arrangement of the components is a self-assembly), and (ii) layer by layer applications of individual components (in this case the components are placed layer by layer).

The protective mechanisms of the developed fluoropolymer coating were explored by the use of different electrochemical techniques, i.e. potentiodynamic measurements and electrochemical impedance spectroscopy in order to study the corrosion behaviour of fluoropolymer coatings on aged quaternary bronze. Contact angle measurement, colour variation after application of the coating and after UV exposure were used to define hydrophobic and colour stability of the coating. Surface sensitive techniques (FIB, EDX/SEM analysis) were used on the coating that exhibited best properties.

## 2. Material and methods

### 2.1. Bronze and simulated patina

Bronze samples were cast in sand moulds having the dimensions  $100\text{ mm} \times 100\text{ mm} \times 5\text{ mm}$ , at a privately-owned foundry. The bronze composition consisted of (Cu to balance): 6.9 Sn, 3.1 Zn and 2.0 Pb in wt.%. This composition is typical of a quaternary as-cast bronze used in an art foundry [19]. It exhibits a classical dendritic structure of an alpha Cu solid solution surrounded by an interdendritic eutectoid which includes a high tin delta phase and immiscible lead globules.

Samples of dimensions  $2.5 \times 5\text{ cm}$  (i.e. working electrodes for the electrochemical experiments) were cut out from the 5 mm thick plates and abraded by means of 4000-grid SiC paper.

The samples were aged by a dropping test for a total Time of Wetness (ToW) of 37 days [20] in order to simulate outdoor exposure in run-off conditions. The preparation of aged patinas in these conditions has been well reported [21–23]. After ageing, the surface macroscopically appears brown-black (Fig. 2a). The important property is that patina achieved by such ageing consists of different corroded regions (Fig. 2 b). The microstructure is changed due to galvanic coupling between the interdendritic and dendritic areas, inducing a decuprification process with a relative increase in the Sn content, as also evidenced in natural outdoor patinas [19]. Typical areas (A to C) are shown in Fig. 2c; they were analysed by Energy dispersive spectrometry (EDS), and the results are reported in Table 1. In the eutectoid area A, the high tin delta phase remains uncorroded, containing only Cu, Sn and Zn elements. Conversely, in the dendritic core corresponding to the copper solid solution with a lower content of tin (area C), the corrosion attack is pronounced. This was revealed by the high dissolution level of copper accompanied by a relative enrichment in tin, and also incorporating important amounts of environmental elements such as O and Cl. Along the eutectoid/dendrite border (area B), the corrosion attack is less pronounced as revealed by the low concentration of oxygen and no detection of other environmental elements such as S and Cl.

### 2.2. Development of the coating

#### 2.2.1. Materials

The methyl methacrylate was provided by Akropol and the 3-

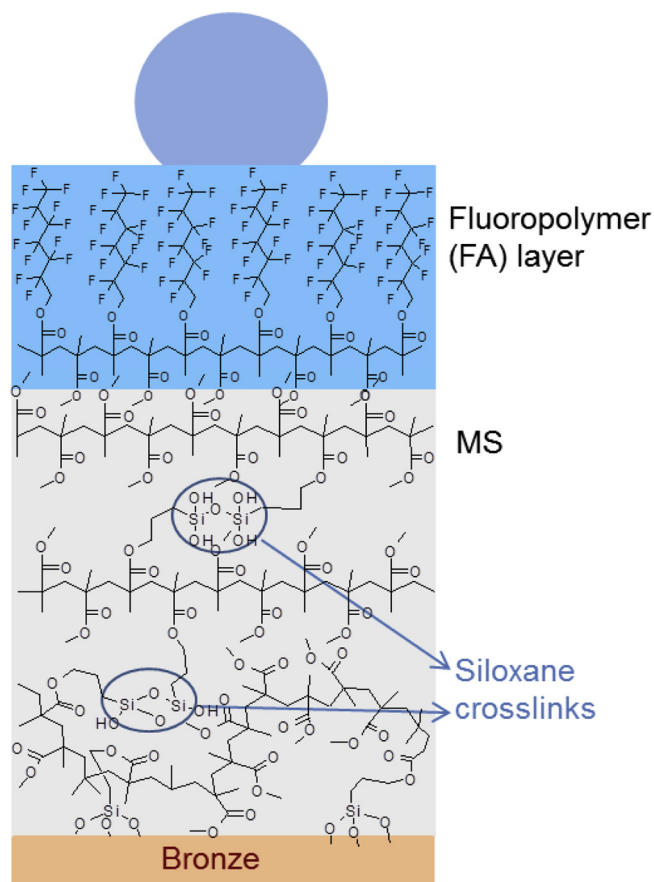


Fig. 1. Schematic presentation of the possible bonding of the proposed multi-component coating to aged bronze.

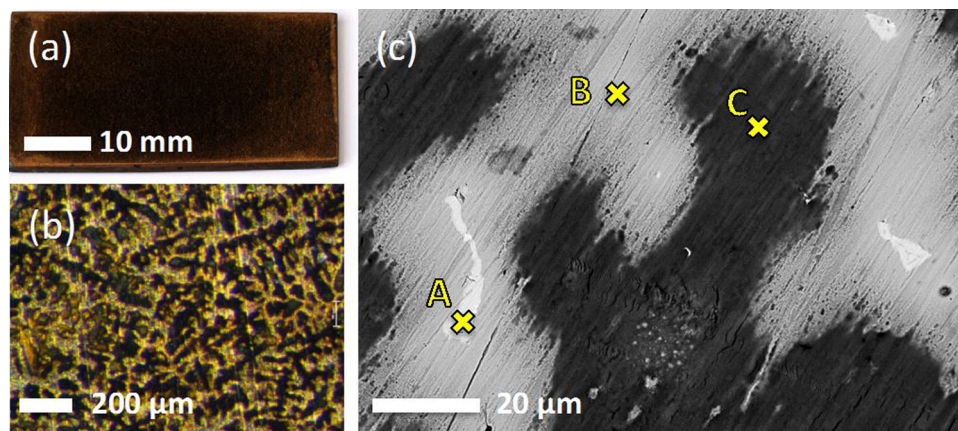


Fig. 2. (a) Macro, (b) optical microscopy observation, and (c) BSE image of the patinated bronze sample (ToW = 37 days).

methacryloxypropyltrimethoxysilane was obtained from ABCR GmbH & Co. As a fluoroacrylate commercial product, Funcosil AG from Remmers was used. Lauroyl peroxide, 3-isocyanatopropyl triethoxysilane, diethyl succinate and *n*-butyl acetate were obtained from Sigma Aldrich. 5-Amino-1H-benzotriazole was purchased from Alfa Aesar and tetrahydrofuran (THF) from Acros Organics. P.A grade acetone was obtained from Honeywell.

### 2.2.2. Syntheses

The individual components of the fluoro-based coating are presented in Fig. 3 and were synthesized as follows:

- a) Adhesion promotor - Random copolymers of methyl methacrylate and methacryloxypropyltrimethoxysilane (9:1 M ratio) - **MS**

The syntheses were performed in a batch reaction. Acetone was used as a solvent and 2% lauroyl peroxide was used as an initiator. The combined monomer concentration was 10% (based on the condensed form of silane). The reaction temperature was 55 °C, and the reaction time was 72 h. After the reaction the diethyl succinate was added to the reaction vessel, and acetone was evaporated at reduced pressure and room temperature to form a 20% solution.

Additional diethyl succinate and *n*-butyl acetate were added to form 5% solution in *n*-butyl acetate and diethyl succinate (1:1 mass ratio) solvent mixture for layer by layer application.

- Fluoroacrylate – **FA**

A commercial solution of a fluoroacrylate was evaporated at 60 °C for several days and redissolved in a mixture of *n*-butyl acetate and diethyl succinate (with a 17:1 mass ratio) to form a 10% solution. Additionally a 5% solution in a mixture of *n*-butyl acetate and diethyl succinate (1:1 mass ratio) was prepared for layer by layer application.

- Silane modified benzotriazole inhibitor - N-5-benzotriazolyl-N'-3-propyltriethoxysilylurea – **BS**

N-5-benzotriazolyl-N'-3-propyltriethoxysilylurea - BS was synthesized by dissolving 0.134 g (1 mmol) of 5-aminobenzotriazole in 3.5 g of dry

THF, and adding 0.248 g (1 mmol) of 3-isocyanatopropyl triethoxysilane. The reaction mixture was left standing for 24 h at room temperature, and then evaporated and dissolved in a mixture of *n*-butyl acetate and diethyl succinate (1:1 mass ratio) to form a 1.5 wt. % solution.

### 2.2.3. Application method

The individual components were applied to the patinated bronze surface by means of two different application techniques by soft brushing (approximately 30 mg of the coating solution). The used application procedures are described below.

In the layer by layer technique (abbreviation LbL), each component of the coating (MS, FA or BS) was separately applied to the bronze surface. A 24 h time interval between each layer application was made, as described hereafter:

- LbL-FA-2MS - Two layers of the 5% MS solution were applied, and then one layer of the 5% FA solution.
- LbL-FA-2MS-BS was obtained by first applying the 1.5% BS solution, then two layers of 5% MS, and finally the 5% FA solution.

In the self-assembled single layer technique, the components of the coating (MS, FA and/or BS) were pre-mixed and then applied to the bronze surface:

- The FA-MS coating was prepared by mixing 1 part of the MS solution and 1 part of the FA solution, forming a 5% FA and 10% MS polymer solution in a 1:1 mass *n*-butyl acetate and diethyl succinate solvent mixture.
- The FA-MS-BS coating was prepared by mixing 1 part of the MS solution and 1 part of the FA solution and dry BS forming a 5% FA, 10% MS polymer, and 1.5% BS solution in a 1:1 mass *n*-butyl acetate and diethyl succinate solvent mixture.

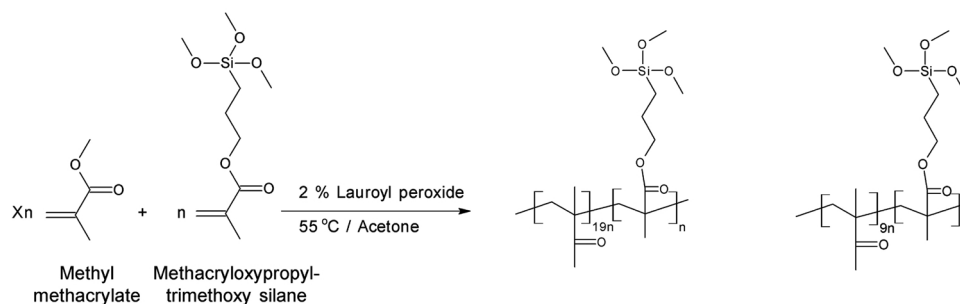
In all cases the coatings were applied to the patinated surface by using a brush, and were left to dry before the measurements began. The coating thicknesses for different application techniques varied from approx. 2 to 3 μm. The electrochemical measurements, contact angle measurements, colour variation before and after UV exposure were

Table 1

Elemental composition of the investigated aged quaternary bronze in wt. %.

area	O	Al	Si	S	Cl	Cu	Zn	Sn	Pb
A (delta phase)	–	–	–	–	–	68 ± 2	0.7 ± 0.2	32 ± 1	–
B (eutectoid/dendrite area)	3 ± 1	–	0.2 ± 0.1	–	–	81 ± 2	2.7 ± 0.2	12.7 ± 0.5	0.4 ± 0.2
C (dendrite centre)	24 ± 1	0.3 ± 0.2	2.5 ± 0.1	0.1 ± 0.1	0.2 ± 0.1	49 ± 2	1.0 ± 0.2	22 ± 2	0.8 ± 0.3

### a) Silane modified poly methylmethacrylate (MS)



### b) Silane modified benzotriazole (BS)

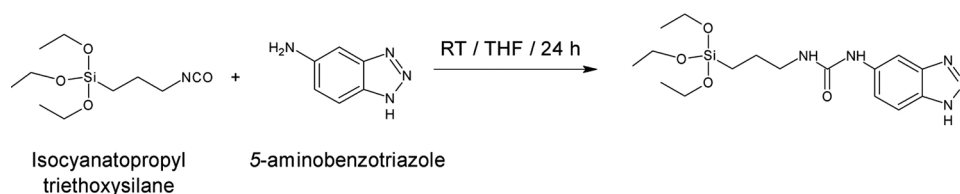


Fig. 3. Scheme of proposed reactions for the synthesis of: (a) the copolymer MS and (b) N-5-benzotriazolyl-N''-3-propyltriethoxysilylurea.

performed on samples before and after the coatings had been freshly applied.

#### 2.3. Measurement of the contact angle, colour variations and exposure in a climate/UV chamber

Contact angle measurements were performed by means of the static method, using the FTA 1000 DropShape Instrument B FrameSystem, First Ten Angstroms. The droplet of distilled water (4  $\mu\text{L}$ ) was placed on the bronze surface and the image was recorded. The static contact angle was defined by fitting the Young – Laplace equation. Measurements were performed at three different areas, and the averaged value was expressed as the result.

Colour variations after the application of the fluoropolymer coating were evaluated using a colorimeter *i1* (X-Rite, USA), operating with a 45/0 measuring geometry illuminant D65 and a 5-mm sample aperture. The total colour change,  $\Delta E^*$ , was calculated from Lab values (CIE 1976 ( $L^*$ ,  $a^*$ ,  $b^*$ ) colour space – CIELAB), measured on the patinated bronze surface before and after applying the polymer layer, using following equation:

$$\Delta E^* = (\Delta L^{*2} + \Delta a^{*2} + \Delta b^{*2})^{1/2} \quad (1)$$

A variation of  $\Delta E^* \leq 3$  cannot usually be distinguished by the naked eye, thus indicating that no significant visual impact of the treatment needs to be reported. Measurements of the colour coordinates at the same areas, before and after the application of the coatings, were performed by using a jig.

The efficiency of protection against UV radiation of the FA-MS coating was evaluated by using the UV radiation of 14.96  $\text{kW h/m}^2$ . The program of the testing was based on the weathering method described in the publication of Chiavari et al. [10]. The test was performed using two climatic chambers: (1) a Q-sun Xe-3 test chamber, Q-lab, and (2) a climatic chamber KK-340 CHLT, Kambič, for obtaining the defined UV and freezing conditions, respectively. The test consisted of 17 cycles, each cycle consisting of four steps: (step 1) a 2 h temperature ramp (from 0  $^\circ\text{C}$  to 35  $^\circ\text{C}$ , the first cycle from room temperature to 35  $^\circ\text{C}$ , with the UV light switched off), (step 2) 16 h of UV exposure (the UV light switched on, the UV irradiance was 55  $\text{W/m}^2$  [24], at T 35  $^\circ\text{C}$  and a relative humidity of 70%), (step 3) a 2 h temperature ramp (from 35  $^\circ\text{C}$

to 0  $^\circ\text{C}$ , with the UV light switched off), and (step 4) 4 h of freezing (4 h at 0  $^\circ\text{C}$ , with the UV light switched off). For these UV exposed samples, visual observation as well as colour variation measurements were performed before and after exposure, as previously described.

#### 2.4. Electrochemical measurements

The electrochemical measurements were performed in a solution which simulated a highly polluted urban environment and contained: 14.4 mg/L  $\text{Ca}_2\text{SO}_4 \cdot 2\text{H}_2\text{O}$ , 15 mg/L  $(\text{NH}_4)_2\text{SO}_4$ , 19.1 mg/L  $\text{NH}_4\text{Cl}$ , 15.1 mg/L  $\text{NaNO}_3$ , 39.3  $\mu\text{L}$  of  $\text{HNO}_3$  65%, 3.2 mg/L  $\text{CH}_3\text{COONa}$  and 0.8 mg/L of  $\text{HCOONa}$ . The pH and conductivity of the prepared solution were 3.3 and  $\sim 345 \mu\text{S/cm}$  respectively. This solution represents 10-fold concentrated acid rain from the Bologna region [21–23], and is designated as "simulated urban acid rain".

A three-electrode corrosion cell was used, with a volume of 22  $\text{cm}^3$ . The working electrode had a surface area of 3.14  $\text{cm}^2$ . For the electrochemical tests a Gamry 600 potentiostat/galvanostat, expanded with a Gamry Instruments framework module, was used. All potentials are reported with respect to the SCE scale.

The screening experiments consisted of a 1-hour stabilization period at open circuit potential (OCP), followed by electrochemical impedance measurements (EIS) using a perturbation voltage signal of 20 mV (rms) applied over the frequency range from 50 to 5 mHz. Seven data points per decade were recorded. This was followed by potentiodynamic measurements. First a cathodic sweep was performed from OCP to  $-0.25 \text{ V}$ , and then an anodic sweep from OCP to  $+0.50 \text{ V}$ , at a scan rate of 0.167 mV/s.

The long-term experiments consisted of consecutive EIS measurements at 1 h, 24 h, 1 day, 3 days, 1 week, and each further week up to 4 weeks. At the end of the experiment, cathodic and anodic potentiodynamic measurements were performed as described above. After each of the EIS measurements in the long-term experiments, the solution was renewed.

The values of the corrosion current from the potentiodynamic experiments,  $j_{\text{corr}}$ , which are given in the tables, are of an informative nature only. They are presented in the Tables in order to numerically illustrate the Figures.

## 2.5. Surface characterisation and spectroscopic analysis

FEI-SEM Helios NanoLab 600i equipment coupled to an EDX system (Aztec Oxford apparatus, SDD detector, WD 4 mm) was used for observations of the fluoropolymer coated patinated bronze. All the samples were carbon nanocoated by sputtering using a Leica ACE 600 for improving conductivity. Surface examinations were performed, and in situ cross sections at specific representative locations were observed. The in situ cross sections were obtained by Focused Ion Beam (FIB) milling ( $\text{Ga}^+$  ions), as detailed in [19]. For the surface and cross-section imaging, an accelerating voltage of 5 kV and a current intensity of 86 pA were used. The EDS X-ray imaging was also performed using an Oxford AZTEC system.

X-ray Photoelectron Spectroscopy (XPS) analyses were carried out on a ThermoScientific K-Alpha system using a monochromated Al-K $\alpha$  source ( $h\nu = 1486.6$  eV). The photoelectron emission spectra were recorded in direct N(Ec). The X-ray spot size was about 400  $\mu\text{m}$  in diameter, whereas the pass energy was fixed at 130 eV with a step of 1 eV for the surveys. Ionic sputtering of the surfaces was performed by means of an  $\text{Ar}^+$  ion beam accelerated under 200 eV at a low current for 30 s, in order to remove carbon surface contamination. The XPS data were fitted by using Thermo Scientific™ Avantage Software, and the Shirley method was used for the background subtraction of all the peaks.

## 3. Results and discussion

First the developed coatings were electrochemically investigated in simulated urban rain, and then the coating was spectroscopically studied.

Four different multi-component fluoro based coatings were investigated, applied to patinated bronze samples. The coatings were applied to the patinated bronze surface using two different techniques: by a "self-assembly" single layer of a mixture of all the components (i.e. the samples FA-MS-BS and FA-MS), and by layer by layer techniques (samples LbL – FA-2MS, LbL- FA-2MS-BS).

### 3.1. Electrochemical tests on the fluoropolymer coatings

The corrosion potential  $E_{\text{corr}}$  and the polarization resistances  $R_p$  of the patinated aged bronze and the different applied coatings are shown in Fig. 4a and b, respectively. The  $R_p$  values were evaluated from the impedance measurements which were performed during the long-term experiment in simulated urban acid rain.

The corrosion potential of the uncoated patinated bronze (i.e. the aged bronze sample) has an initial value of 0.003 V and increases slowly up to 0.10 V, after 4 weeks of immersion. The increase in the potential

accounts for the possible growth of an oxide film, i.e.  $\text{Cu}_2\text{O}$ . The different protection systems (coated patinated bronze) exhibited different starting corrosion potentials at a 1 h exposure. The most stable corrosion potential occurred in the case of FA-MS, which stayed at around 0.045 V, whereas in the case of FA-MS-BS there were fluctuations in the corrosion potential, indicating the instability of the coating during the 1 month exposure period.

The evolution of polarization resistance over time, evaluated from the impedance data of the different fluoropolymer coatings, is presented in Fig. 4b. These results were derived from the raw impedance data (Supplementary-Table 1) by means of the selected fitting procedure using one or two time constants.  $R_p$  values were estimated as the sum of partial resistances, subtracted by solution resistance.

The polarization resistance for coated samples values evaluated from the impedance values which were close to  $1 \text{ M}\Omega \text{ cm}^2$  are much higher when compared to the values for the uncoated aged bronze sample. The FA-MS coating showed the highest  $R_p$  values, with a value of  $5.6 \text{ M}\Omega \text{ cm}^2$  at the end of 1 month exposure. The long term behaviour of FA-MS is very stable. Also, FA-MS-BS showed good performance during 1 month exposure, with values of  $1.8 \text{ M}\Omega \text{ cm}^2$ . The LbL-FA-2MS-BS experienced a drop in impedance after 3 and 4 weeks of exposure, whereas the LbL-FA-2MS was stable throughout the exposure period with an impedance value of  $1.2 \text{ M}\Omega \text{ cm}^2$  after 1 month of exposure. Among the tested fluoropolymer coatings on aged bronzes, the FA-MS showed the best performance.

The potentiodynamic behaviour of the five different coatings applied to aged patinated bronze test specimens is presented in Fig. 5. The  $j_{\text{corr}}$  values were determined from the polarization measurements which were performed after 1 month of exposure.

A slight variation in the estimated  $E_{\text{corr}}$  observed for the aged bronze and the differently coated aged bronze was observed (Fig. 5). The uncoated aged bronze underwent rapid dissolution, as can be seen from the large increase in current density on the potentiodynamic curve (Fig. 5) with  $j_{\text{corr}}$  of  $1.95 \mu\text{A}/\text{cm}^2$ . The different protective coatings affected both cathodic and anodic polarization, as can be seen from the decrease in the cathodic and anodic current densities in the different parts of the potentiodynamic scans. The largest decrease in cathodic current densities was observed in the case of the FA-MS fluoropolymer coating. As well as this, the anodic current densities are lower in comparison to the uncoated aged bronze in the potential region from 0.0 V to 0.4 V. Not very typical passive regions can be observed, but the anodic current densities are much lower than in the case of the aged patinated bronze. The lowest anodic current density was observed in the case of the FA-MS-BS coating with benzotriazole acting as anodic type of inhibitor. In the case of this coating  $j_{\text{corr}}$  amounted to  $0.0065 \mu\text{A}/\text{cm}^2$ , whereas in the case of the FA-MS coating it was the lowest, with an estimated value of  $0.002 \mu\text{A}/\text{cm}^2$ . The layer by layer

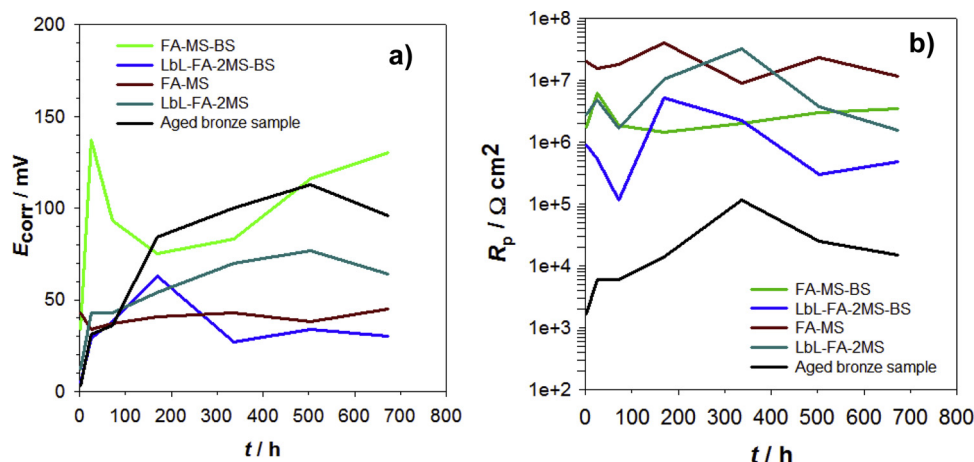


Fig. 4. (a)  $E_{\text{corr}}$  and (b)  $R_p$  results in the case of the fluoropolymer coatings on aged bronze during 1 month of exposure in simulated urban acid rain.

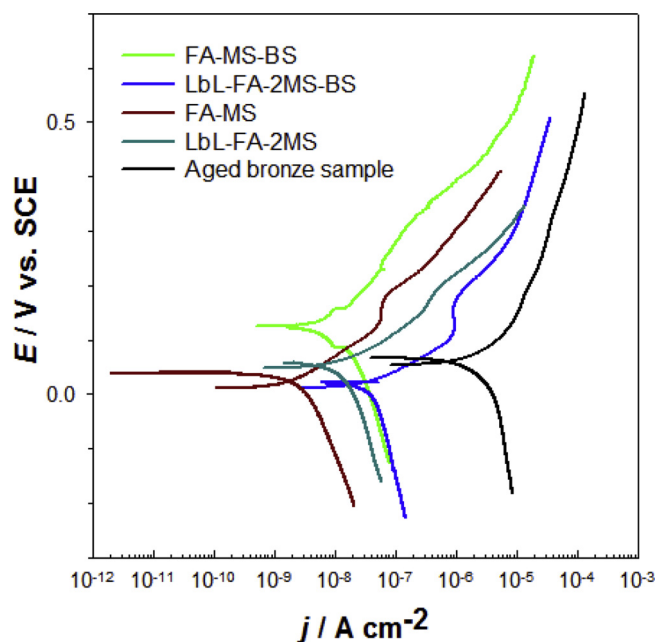


Fig. 5. Cathodic and anodic curves for the aged bronze sample and different applications of fluoropolymer coatings in simulated urban acid rain, scan rate 1 mV/s.

application method proved to be efficient with  $j_{\text{corr}}$  0.015  $\mu\text{A}/\text{cm}^2$  for LbL-FA-2MS, and 0.039  $\mu\text{A}/\text{cm}^2$  for LbL-FA-2MS-BS, but less than the previously observed coatings. This means that better corrosion behaviour was observed in the case of the FA-MS coating, when compared to FA-MS-BS coating with benzotriazole. It is also clearly seen that the single application exhibits better efficiency, by a factor of ten, than the layer by layer application.

### 3.2. Hydrophobicity and colour variations

The results of contact angle measurements and colour variations are presented in Table 2. The contact angle with water for bare bronze was 68°, whereas the values obtained after the fluoropolymer coating had been applied to the samples were between 102° and 116°. This suggests the formation of a hydrophobic surface after the application of the fluoropolymer.

The changes in the colour of the samples after the application of the different fluoropolymers cannot be distinguished by the naked eye (Table 2). The results of the visual observations are in good agreement with those obtained by measurements of the total colour change on the basis of CIE 1976 ( $L^*$ ,  $a^*$ ,  $b^*$ ) colour space. Actually, the  $\Delta E^*$  values for all the samples were less than or equal to 1. Additionally, according to the report by Mokrzycki et al. [25], no colour difference can be distinguished since the  $\Delta E^*$  has a value of less than 1. So it can be concluded that the application of the selected fluoropolymers does not affect the colour properties of the patinated bronze. Apart from this, the FA-MS coating remained transparent, and its colour did not change in

Table 2

Measured contact angles and total colour change of the FA-MS-BS, LbL-FA-2MS-BS, FA-MS and LbL-FA-2MS samples.

Coating	Contact angle/ $^\circ$	Total colour change after application of the coating ( $\Delta E^*$ )
Aged bronze	68	/
FA-MS	108	< 1
FA-MS-BS	116	< 1
LbL-FA-2MS	109	< 1
LbL-FA-2MS-BS	102	< 1

the case of UV exposure and thermal cycling ( $\Delta E^* = 1$ ).

### 3.3. Properties of the fluoropolymer FA-MS coating

According to the above already-mentioned results, when the FA-MS fluoropolymer coating was deposited on the patinated bronze surface as a "self-assembly" single layer (i.e. as a mixture of the FA and MS components) better protective behaviour against corrosion was observed, as well as no colour modification. For this reason this type of coating appears to have the best properties, as well as being the most adequate candidate for outdoor bronze protection. The results of the microscopy investigation by FEG-SEM are presented in Fig. 6. It can be seen that the coating covers the surface of the patinated bronze evenly (Fig. 6a); such even covering the corrosion structure being previously evidenced in Fig. 2, and the imperfections were microscopically defined as corrosion areas at the dendrite centres [20]. Except for a few microporosities observed as micro-bubbles, the coating layer is dense and has good adherence (Fig. 6b). From the FIB cross-section, the average thickness of the coating was determined to be about 2  $\mu\text{m}$  (Fig. 6b-d), independently of the patina thickness, which could be very thin as revealed in the case of the eutectoid area (Fig. 6c), or thick in the case of the centre of the dendrite (Fig. 6d). A developed network of nanoporosities was observed within the artificial patina which can be linked to the phenomenon of decuprification and agrees well with observations of outdoor bronze impacted by direct exposure to acid rain [19].

The elemental distribution within the coating/patina/bronze system can be seen from the X-ray maps performed across the FIB cross-section, which are presented in Fig. 7. The coating layer is not uniform in composition. In particular, the F element was detected in the internal part of the polymer, coupled with intense C and O signals. This chemical inhomogeneity supports the idea of using several polymers in this formulation since it reveals that the application of such a coating permits diffusion within the patina, significantly improving wettability performance. This was observed for all the coating elements (C, F and Si). This result confirms the good ability of this coating to affect the entire surface including the patina, which explains its very good coverage quite independently of the patina thickness.

XPS was performed in order to better determine the chemical structure of the formed fluoropolymer top layer on the patinated bronze. The XPS survey spectra before and after Ar + etching 30 s at 200 eV are presented in Fig. 8. The atomic quantification of the FA-MS coating is reported in Table 3. From the results of the XPS profile spectra, it can be seen that, before etching, the upper outer part of the layer consists mainly of the elements C, O and F. From the results of the XPS survey after etching, it was concluded that the FA-MS polymer is very sensitive to this decontamination step. The very slight Ar + sputtering induced a chemical modification of the top surface, revealed by a variation in the intensity and position of some element peaks. As is shown Table 4, this is proved by a variation in the O 1 s signal, and a pronounced decrease in the F content, whereas the C 1 s peaks are intensified, but with a loss of C–F binding. Thus part of the fluor (5.6 at. %) is related to a redeposition of F after stripping/etching of the extreme surface.

Thus only the quantitative data obtained before etching have to be taken into account (Table 3). With respect to the C 1 s peak, two peaks at 291.4 eV and 293.8 eV, corresponding mainly to C–F2 and C–F3 respectively [26], were observed, which is in agreement with the atomic C/F ratio.

The Si content remains very low at the limit of detection, but even if the Si 2p peak is poorly resolved, the peak value at 101.9 eV can be attributed to the Si–O–Si bonds in the polysiloxane.

From the results of the XPS investigations, it can be concluded that a protective mechanism formed on aged bronze is dependent on a chemisorbed layer, which is achieved by bonding to copper and tin with the formation of hydrogen and metal-siloxane bonding [27–29]. Over the crosslinked part of the coating of a siloxane layer, it is assumed that

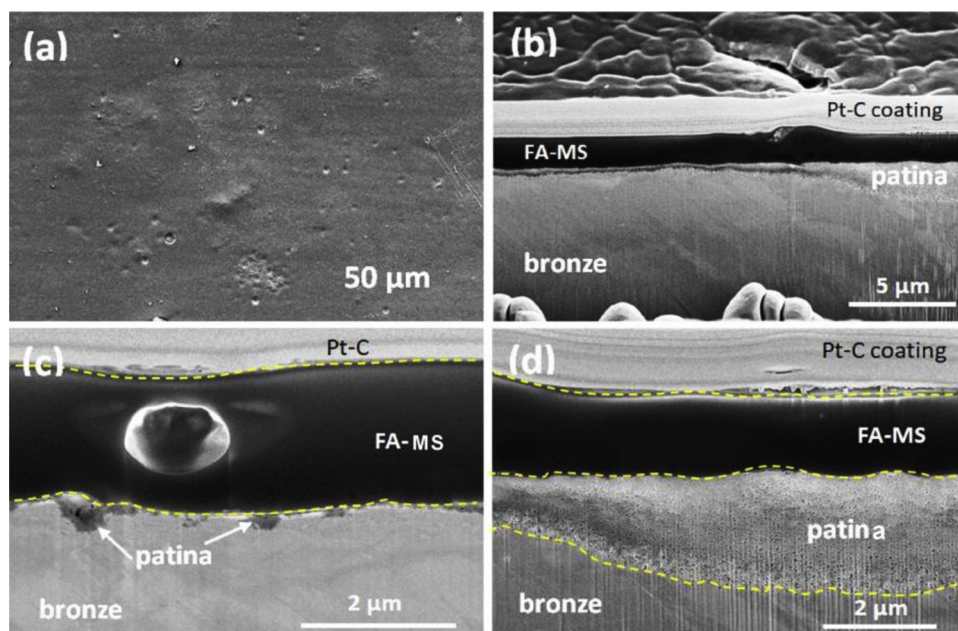


**Fig. 6.** SEM images of the FA-MS coated surface on patinated as-cast bronze. (a) Surface observation and FIB milling cross-section of: (b) global observation, (c and d) detailed views of respectively (c) the bronze eutectoid area (a very thin patina layer) and (d) the dendrite centre (a thick patina layer with nanoporosities).

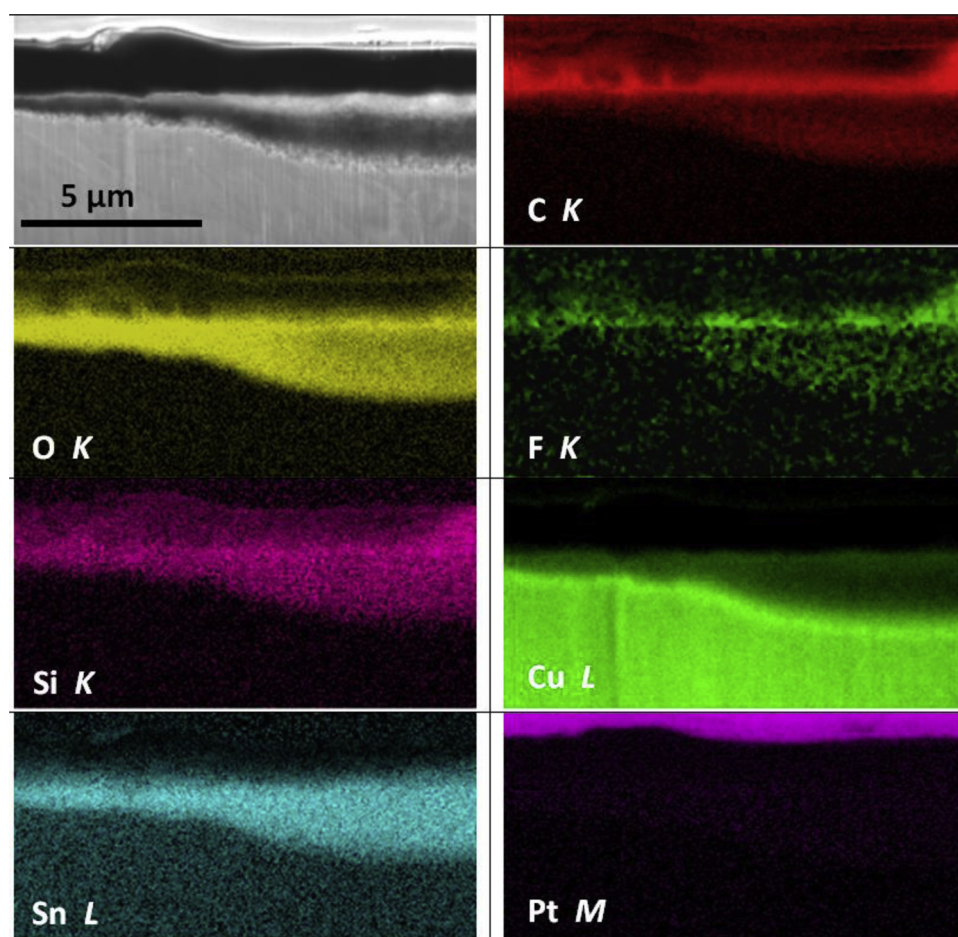


**Fig. 7.** X-ray maps of the FA-MS coated pre-patinated sample centred in the corroded layer (SE image, C, O, F, Si, Cu, Sn and Pt).

fluoroacrylate part is adsorbed via dipole interactions of ester groups, and hydrophobic interactions, as well as by the entanglement of polymer chains. This outer part shows hydrophobic properties.

According to the results presented in Table 3, the contact angle of the aged bronze changed from 68° to 108° for the FA-MS coating. This mechanism is schematically presented in Fig. 1.

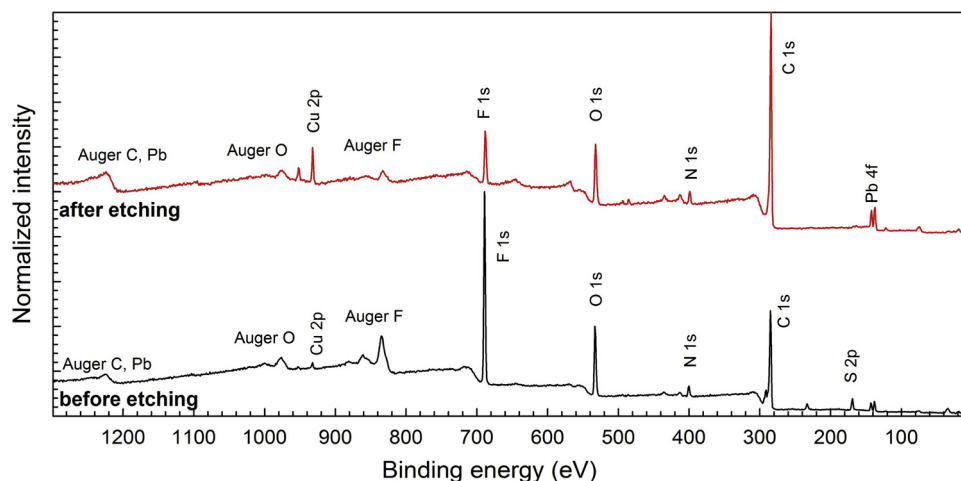


Fig. 8. XPS profile spectra of the FA-MS fluoropolymer coating before and after Ar<sup>+</sup> etching (30 s, 200 eV).

Table 3

Bending energies (eV) and atomic quantification (at%) in the obtained XPS spectra before and after the Ar<sup>+</sup> etching.

	C 1s					N 1s	O 1s	F 1s	Si2p	S 2p	sulphate
	CC, CH	C-O, CN	O = C-O	C-F <sub>2</sub>	C-F <sub>3</sub>	CN CNH		C-Fx	Si-O-Si	C-S-C	
Before etching											
Peak BE (eV)	284.7	286.4	288.8	291.4	293.8	400.0	532.8	688.6	101.9	163.2	168.8
at%	40.7	13.4	4.1	5.2	1.5	3.3	16.2	13.3	< 0.1	–	2.4
After etching											
Peak BE (eV)	284.3	286.0	288.4	291.5	293.9	399.5	532.0	688.0	102.5	163.0	167.9
at%	63.8	12.0	3.9	–	–	2.9	11.0	5.6	0.2	0.2	0.3

The results of the electrochemical studies which were performed over a period of 1 month using simulated urban acid rain showed that the developed fluoropolymer with adhesion promoter (FA-MS) substantially improved the polarization resistance of the aged patinated bronze. Even though this coating is only a few  $\mu\text{m}$  thick, it provides good protection. The coating does not change after ageing by immersion in urban acid rain, as well as remaining transparent, and maintaining its protective properties.

#### 4. Conclusions

Multi-component fluoropolymer based coatings for aged bronze were developed, and their electrochemical behaviour was studied in simulated urban acid rain in order to assess their protective efficiency. Different application techniques of fluoropolymer coatings were evaluated. The following conclusions were drawn:

- The FA, MS and BS components were investigated on bronze, which had been aged in simulated outdoor conditions; different application methods of components were used such as layer by layer technique and single-layer mixture of all components.
- The results of electrochemical impedance spectroscopy measurements over a 4-week exposure period showed that FA and MS components, when applied as a single-layer mixture of its two components (FA-MS), behaved in the most stable manner, and resulted in very high polarization resistances during this exposure period.
- The coating FA-MS also has high hydrophobicity, smoothly covers the surface of aged bronze, and does not change in colour either when applied or after aging in a UV/climatic chamber.
- The fluoropolymer coating FA-MS as such exhibits excellent protective and durable protection for aged bronze in outdoor conditions.

#### Acknowledgements

This work was performed within the scope of the M-ERA.NET European project B-IMPACT project (2015–2017), within the M-ERA.NET network, and supported by national funding organizations (MIZS-Slovenia, MIUR-Italy, RMP- France).

The raw/processed data required to reproduce these findings cannot be shared at this time as the data also forms part of an ongoing study.

#### Appendix A. Supplementary data

Supplementary material related to this article can be found, in the online version, at doi:<https://doi.org/10.1016/j.porgcoat.2019.01.040>.

#### References

- [1] P.A. Schweitzer, *Fundamentals of Metallic Corrosion: Atmospheric and Media Corrosion of Metals*, Corrosion Engineering Handbook, 2nd ed., CRC press, Taylor & Francis Group, NY, 2007.
- [2] V.N. Naudé, *Guide to the Maintenance of Outdoor Sculpture*, American Institute for Conservation of Historic and Artistic Works, Washington, D.C, 1993.
- [3] A. Galtayries, A. Mongiatti, P. Marcus, C. Chiavari, Surface characterisation of corrosion inhibitors on bronzes for artistic casting, in: P. Dillmann, G. Beranger, P. Piccardo, H. Matthiesen (Eds.), *Corrosion of Metallic Heritage Artefacts*, Woodhead Publishing Limited, Cambridge, 2007, p. 335.
- [4] L. Muresan, S. Varvara, E. Stupnišek-Lisac, H. Otmačić, K. Marušić, S. Horvat-Kurbegović, L. Robbiola, K. Rahmouni, H. Takenouti, Protection of bronze covered with Patina by innocuous organic substances, *Electrochim. Acta* 52 (2007) 7770–7779.
- [5] R. Bostan, S. Varvara, L. Găină, T. Petrisor, L.M. Mureşan, Protective effect of inhibitor-containing nitrocellulose lacquer on artificially patinated bronze, *Prog. Org. Coat.* 111 (2017) 416–427.
- [6] C.J. McNamara, M. Breuker, M. Helms, T.D. Perry, Ralph Mitchell Biodeterioration of Infracalac used for the protection of bronze monuments, *J. Cult. Herit.* 5 (2004) 361–364.
- [7] K. Rahmouni, H. Takenouti, N. Hajjaji, A. Srhiri, L. Robbiola, Protection of ancient and historic bronzes by triazole derivatives, *Electrochim. Acta* 54 (2009) 5206–5215.
- [8] T. Kosec, H. Otmačić Čurković, A. Legat, Investigation of the corrosion protection of

- chemically and electrochemically formed patinas on recent bronze, *Electrochim. Acta* 56 (2010) 722–731.
- [9] G. Brunoro, A. Frignani, A. Colledan, C. Chiavari, Organic films for protection of copper and bronze against acid rain corrosion, *Corros. Sci.* 45 (2003) 2219–2231.
- [10] C. Chiavari, A. Balbo, E. Bernardi, C. Martini, C. Monticelli, Organosilane coatings applied on bronze: influence of UV radiation and thermal cycles on the protectiveness, *Prog. Org. Coat.* 82 (2015) 91–100.
- [11] P. Ropret, T. Kosec, Raman investigation of artificial patinas on recent bronze - part I: climatic chamber exposure, *J. Raman Spectrosc.* 43 (2012) 1578–1586.
- [12] G. Bierwagen, T.J. Shedlosky, K. Stanek, Developing and testing a new generation of protective coatings for outdoor bronze sculpture, *Prog. Org. Coat.* 48 (2003) 289–296.
- [13] B. Salvadori, A. Cagnini, M. Galeotti, S. Goidanich, A. Vincenzo, C. Celi, P. Frediani, L. Rosi, M. Frediani, G. Giuntoli, L. Brambilla, R. Beltrami, S. Trasatti, Traditional and innovative protective coatings for outdoor bronze: application and performance comparison, *J. Appl. Polym. Sci.* 135 (46011) (2018) 1–12.
- [14] A. Skaja, Testing coatings for zebra and quagga mussel control, *J. Protect. Coat. Linings* 27 (2010) 57–65.
- [15] A. Brooks, G. Hennighan, S. Woollard, Von Werne, A Plasma Deposited Surface Finish for Printed Circuit Boards (Conference Paper), T.IPC APEX EXPO 2012 Volume 3, 2012, Pages 2106–2124 IPC APEX EXPO 2012; San Diego, CA; United States; 28.2.2012 -1.3, (2012) Code 93352.
- [16] J.L. Yagüe, P. Segadó, M. Auset, S. Borrós, Textured superhydrophobic films on copper prepared using solvent-free methods exhibiting antifouling properties, *Thin Solid Films* 635 (2017) 32–36.
- [17] Y. He, D. Walsch, C. Shi, Fluoropolymer composite coating for condensing heat exchangers: characterization of the mechanical, tribological and thermal properties, *Appl. Ther. Eng* 91 (2015) 387–398.
- [18] S. Ebnesajjad, *Applied Plastics Engineering Handbook (4: Introduction to Fluoropolymers)*, Elsevier Inc., 2011.
- [19] C. Chiavari, K. Rahmouni, H. Takenouti, S. Joiret, P. Vermaut, L. Robbiola, Composition and electrochemical properties of natural patinas of outdoor bronze monuments, *Electrochim. Acta* 52 (2007) 7760–7769.
- [20] G. Masi, J. Esvan, C. Josse, C. Chiavari, E. Bernardi, C. Martini, M.C. Bignozzi, N. Gartner, T. Kosec, L. Robbiola, Characterization of typical patinas simulating bronze corrosion in outdoor conditions, *Mater. Chem. Phys.* 200 (2017) 308–321.
- [21] E. Bernardi, C. Chiavari, B. Lenza, C. Martini, L. Morselli, F. Ospitali, et al., The atmospheric corrosion of quaternary bronzes: the leaching action of acid rain, *Corros. Sci.* 51 (2009) 159–170, <https://doi.org/10.1016/j.corsci.2008.10.008>.
- [22] C. Chiavari, E. Bernardi, A. Balbo, C. Monticelli, S. Raffo, M.C. Bignozzi, et al., Atmospheric corrosion of fire-gilded bronze: corrosion and corrosion protection during accelerated ageing tests, *Corros. Sci.* 100 (2015) 435–447, <https://doi.org/10.1016/j.corsci.2015.08.013>.
- [23] E. Bernardi, C. Chiavari, C. Martini, L. Morselli, The atmospheric corrosion of quaternary bronzes: an evaluation of the dissolution rate of the alloying elements, *Appl. Phys. A Mater. Sci. Process.* 92 (2008) 83–89, <https://doi.org/10.1007/s00339-008-4451-0>.
- [24] ISO 4892-2, *Plastics – Methods of Exposure to Laboratory Light Sources – Part 2: Xenon-arc Lamps*, (2013).
- [25] W.S. Mokritzky, M. Tatol, Colour difference Delta e - a survey, *Mach. Graph. Vis.* 20 (2011) 383–412.
- [26] Ch. Cardinaud, A. Rhouma, G. Turban, B. Grolleau, Polymerisation et gravure en plasma fluorocarboné, *Revue Phys. Appl.* 24 (1989) 309–321.
- [27] L. Picard, P. Phalip, E. Fleury, F. Ganachaud, Chemical adhesion of silicone elastomers on primed metal surfaces: a comprehensive survey of open and patent literatures, *Prog. Org. Coat.* 80 (2015) 120–141, <https://doi.org/10.1016/j.porgcoat.2014.11.022>.
- [28] C. Chiavari, A. Balbo, E. Bernardi, C. Martini, M.C. Bignozzi, M. Abbottoni, C. Monticelli, Protective silane treatment for patinated bronze exposed to simulated natural environments, *Mater. Chem. Phys.* 141 (2013) 502–511, <https://doi.org/10.1016/j.materchemphys.2013.05.050>.
- [29] G. Masi, A. Balbo, J. Esvan, C. Monticelli, J. Avila, L. Robbiola, et al., X-ray Photoelectron Spectroscopy as a tool to investigate silane-based coatings for the protection of outdoor bronze : the role of alloying elements, *Appl. Surf. Sci.* (2017), <https://doi.org/10.1016/j.apsusc.2017.10.089>.